



HAL
open science

Effect of a northward turning of the interplanetary magnetic field on cusp precipitation as observed by Cluster

P. Escoubet, J. Berchem, Jean-Michel Bosqued, K. J. Trattner, M. G. Taylor, Frederic Pitout, H. Laakso, Arnaud Masson, M.W. Dunlop, I. Dandouras, et al.

► To cite this version:

P. Escoubet, J. Berchem, Jean-Michel Bosqued, K. J. Trattner, M. G. Taylor, et al.. Effect of a northward turning of the interplanetary magnetic field on cusp precipitation as observed by Cluster. *Journal of Geophysical Research Space Physics*, 2008, 113 (A7), pp.A07S13. 10.1029/2007JA012771 . insu-00360347

HAL Id: insu-00360347

<https://insu.hal.science/insu-00360347>

Submitted on 2 Aug 2021

HAL is a multi-disciplinary open access archive for the deposit and dissemination of scientific research documents, whether they are published or not. The documents may come from teaching and research institutions in France or abroad, or from public or private research centers.

L'archive ouverte pluridisciplinaire **HAL**, est destinée au dépôt et à la diffusion de documents scientifiques de niveau recherche, publiés ou non, émanant des établissements d'enseignement et de recherche français ou étrangers, des laboratoires publics ou privés.

Copyright

Effect of a northward turning of the interplanetary magnetic field on cusp precipitation as observed by Cluster

C. P. Escoubet,¹ J. Berchem,² J. M. Bosqued,³ K. J. Trattner,⁴ M. G. G. T. Taylor,¹ F. Pitout,⁵ H. Laakso,¹ A. Masson,¹ M. Dunlop,⁶ I. Dandouras,³ H. Reme,³ A. N. Fazakerley,⁷ and P. Daly⁸

Received 27 August 2007; revised 19 October 2007; accepted 8 January 2008; published 2 May 2008.

[1] The immediate effect of the rotation of the interplanetary magnetic field (IMF) from southward to northward on cusp precipitation has been rarely observed by a polar orbiting satellite in the past. The four Cluster spacecraft observed such an event on 23 September 2004 as they were crossing the polar cusp within 2–16 min from each other. Between the first three and the last spacecraft crossing the cusp, the IMF rotated from southward to northward with a dominant By (GSM) component. For the first time we can examine the changes in the particle precipitation immediately after such IMF change. The first two spacecraft observed typical IMF-southward ion dispersion, while the last one observed both an IMF-southward-like dispersion in the boundary layer and an IMF-northward dispersion in the cusp. After the IMF turning, the cusp is shown to have grown in size in both the poleward and equatorward directions. A three-dimensional magnetohydrodynamic simulation is used to determine the locations of the sources of the ions and the topology of the magnetic field during the event.

Citation: Escoubet, C. P., et al. (2008), Effect of a northward turning of the interplanetary magnetic field on cusp precipitation as observed by Cluster, *J. Geophys. Res.*, 113, A07S13, doi:10.1029/2007JA012771.

1. Introduction

[2] First observations of the polar cusp were obtained by *Heikkila and Winningham* [1971] and *Frank* [1971], more than 35 years ago. Since that time, many studies have investigated the numerous physical processes occurring in the cusp such as particle injections, and the generation of currents and broadband waves, as well as the dynamics of the cusp itself. Being the region of the magnetosphere with one boundary at the magnetopause and the other one in the ionosphere, the polar cusp has been explored by high-, middle- and low-altitude spacecraft, as well as from the ground.

[3] Since *Burch* [1973] first identified the dependence of the magnetospheric cusp location on the magnitude of the B_Z component of the interplanetary magnetic field (IMF), there have been many observational studies of the response

of the cusp to changes in solar wind. Although a few early studies considered the effects of currents induced by substorms [*Eather*, 1985], it is now well established that the IMF orientation and solar wind dynamic pressure exert a strong effect on the structure and dynamics of the cusp [e.g., *Carbary and Meng*, 1986; *Escoubet and Bosqued*, 1989; *Woch and Lundin*, 1992; *Newell and Meng*, 1994; *Sandholt et al.*, 1994; *Zhou et al.*, 2000; *Bosqued et al.*, 2005; *Pitout et al.*, 2006a, 2006b].

[4] Cusp particle precipitation has been extensively studied, with ion energy dispersion signatures providing a useful indication of the process by which particles enter into the polar cusp. *Reiff et al.* [1977] proposed the first models to explain the ion energy dispersion: one focused on magnetic merging to explain the decrease of the ion energy with increasing latitude; the other described cross-field diffusion as a means to explain V-shaped (a decrease of energy followed by an increase as latitude increases) dispersions. Later on, *Reiff et al.* [1980] demonstrated that the merging signatures were occurring for IMF southward and the V-shaped signatures for IMF northward. *Burch et al.* [1980] established a clear distinction between the equatorward part of the “V” and the poleward part: the equatorward side showed a strong eastward and anti-sunward flow while the poleward part had a low eastward but significant sunward component. *Newell and Meng* [1991] and *Woch and Lundin* [1992] further distinguished the ion dispersion into two parts: accelerated magnetosheath plasma on the high-energy side and typical magnetosheath plasma on the low-energy side. Acceleration was shown to occur on the equatorward side of the cusp for southward IMF and either on the

¹European Space Research and Technology Centre, European Space Agency, Noordwijk, Netherlands.

²Institute of Geophysics and Planetary Physics, University of California, Los Angeles, California, USA.

³Centre d’Etude Spatiale des Rayonnements, Toulouse, France.

⁴Lockheed Martin Air Traffic Management, Palo Alto, California, USA.

⁵Laboratoire de Planetologie de Grenoble, Saint-Martin d’Heres, France.

⁶Rutherford Appleton Laboratory, Didcot, UK.

⁷Department of Physics, Mullard Space Science Laboratory, University College London, Dorking, UK.

⁸Max Planck Institute for Solar System Research, Katlenburg-Lindau, Germany.

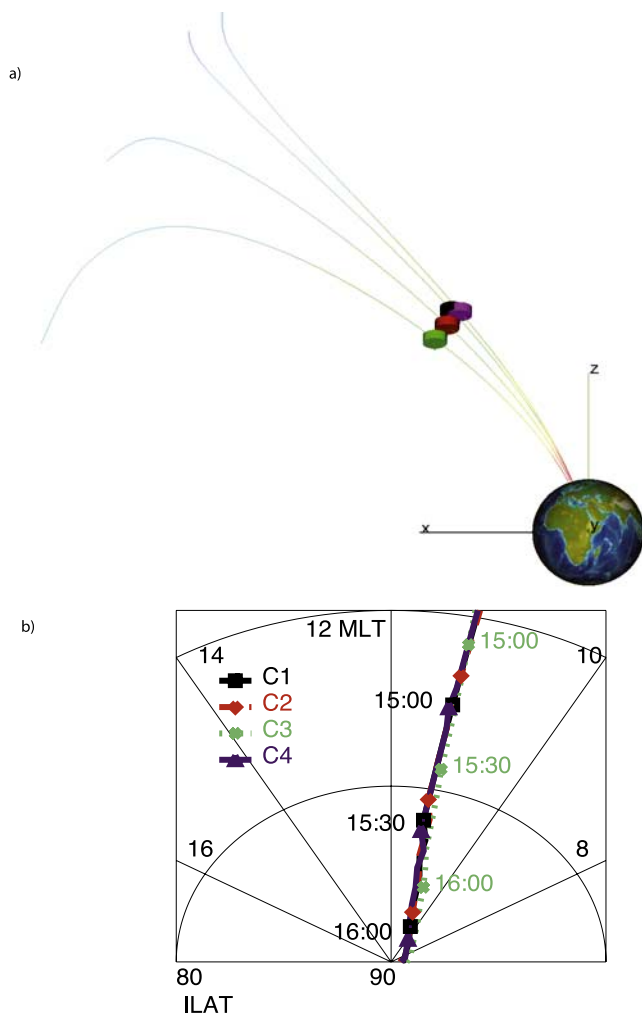


Figure 1. (top) Cluster orbit in GSE XZ plane at 1530 on 23 September 2004 and (bottom) projection of orbit track in ILAT-MLT diagram. The colors of the spacecraft are the usual Cluster colors (C1, black, C2, red, C3, green, and C4, magenta). The time delays and the separations of the spacecraft in latitude are $dt_{41} = 2$ min, $dt_{42} = 8$ min, $dt_{43} = 16$ min and $dlat_{41} = 0.4^\circ$, $dlat_{42} = 1.9^\circ$, $dlat_{43} = 3.7^\circ$.

poleward side or on both equatorward and poleward sides for IMF northward [Woch and Lundin, 1992].

[5] Most of the previous studies have studied the cusp under IMF northward or southward conditions separately. In fact only on rare occasions the cusp was observed by satellite during a change in the IMF orientation. Yamauchi *et al.* [1995] found only one cusp observation in the Viking database when the IMF changed from southward to northward. They initially observed a typical injection for southward IMF and then a second one poleward, with no clear dispersion, associated with northward IMF. However, because the IMF returned quickly to its initial southward direction, they could not determine the southward change associated with the first injection and they had to suggest two different scenarios [Yamauchi *et al.*, 1995].

[6] With Cluster, the ability to investigate changes in the cusp characteristics associated with transitions in the direction of the IMF is greatly improved due to (1) each

spacecraft spending a longer time in the cusp (typically 15–20 min) at around 4–5 R_e altitude and (2) the four Cluster spacecraft follow each other as a string of pearls, in the vicinity of the midaltitude cusp, with a few minutes to a few hours time delay, depending on the yearly separation distance. The cusp can therefore be observed for a longer time and be resolved temporally and spatially instantaneously with more than one spacecraft. Trattner *et al.* [2003] described an example of midaltitude cusp crossing where the ion structures were in agreement with the convection cells observed from the ground and concluded that the structures were spatial. In a later study, Trattner *et al.* [2005a] found another case where the cusp structure was clearly temporal and moving within the same convection cell as first proposed by Escoubet *et al.* [1992] and Lockwood and Smith [1992]. Bosqued *et al.* [2005] analyzed three injections observed in the cusp using Cluster and IMAGE during a period of high solar wind pressure and suggested that the pressure pulses were changing the reconnection rate at the magnetopause. Pitout *et al.* [2006a] studied the fast response of the cusp (within minutes) to three rotations of the IMF and deduce that the speed of the cusp boundaries was around 30 km/s. More recently, Escoubet *et al.* [2006] identified the evolution of an ion energy step into a full dispersion a few minutes after a southward turning of the IMF. A following study [Escoubet *et al.*, 2008] suggested that under southward IMF with a strong B_y component, two sources of magnetosheath ion existed simultaneously, one in the frontside of the magnetosphere triggered by component reconnection taking place near the subsolar region and one in the dusk flank, resulting from the occurrence of antiparallel reconnection in that region.

[7] In this study we analyze a cusp crossing during an isolated turning of the IMF from southward to northward. The first two Cluster spacecraft crossed the cusp when the IMF was southward, the third one during the turning, and the last spacecraft when the IMF was northward. Ions and electrons measured by the Cluster spacecraft are used to investigate the properties of the source populations and a three-dimensional magnetohydrodynamic (MHD) simulation is used to understand the global response of the magnetosphere and the location of the cusp sources.

2. Observations

2.1. Cluster Orbit and Instrumentation

[8] The Cluster mission comprises of four identical spacecraft that were launched in two pairs onboard a Soyuz rocket in July and August 2000 [Escoubet *et al.*, 2001]. The four spacecraft orbits are optimized to form a tetrahedron usually around the apogee, in the plasma sheet or in the magnetopause/exterior cusp. Near perigee due to orbital mechanics, the tetrahedron is deformed and the spacecraft follow each other in a string of pearl configuration at the same local time. In summer 2004, the tetrahedron size was 1000 km in the tail and the time delay between the four spacecraft at perigee was around a few minutes. This study uses data from the ion spectrometer CIS [Reme *et al.*, 2001], electron detector PEACE [Johnstone *et al.*, 1997], and energetic electrons RAPID instrument [Wilken *et al.*, 2001].

[9] Figure 1 displays the Cluster spacecraft position in the midaltitude cusp on 23 September 2004. The four spacecraft

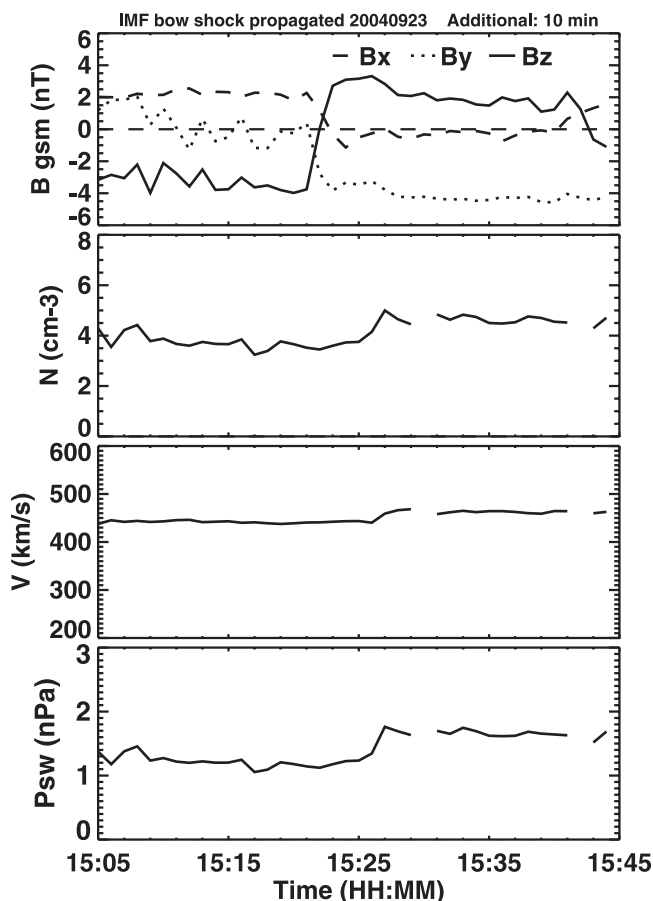


Figure 2. Solar wind conditions on 23 September 2004 from the ACE spacecraft, propagated to the bow shock (Omniweb). Another shift of 10 min was applied to the data to take into account the propagation from the bow shock to the midaltitude cusp.

crossed the polar cusp between 1510 and 1540 UT at an altitude of 4–5 R_E . Their position at 1515 UT is shown in XZ_{GSE} coordinate system on Figure 1a. The *Tsyganenko and Stern* [1996] magnetic field model has been used to trace field lines passing by each spacecraft. C4 (magenta) was leading, followed by C1 (2 min later), C2 (8 min later) and finally C3 (16 min later). Figure 1b shows the track of each spacecraft projected in a ILAT-MLT diagram. It is clear from Figure 1b that all four spacecraft follow one another around 11.2 h MLT. At 1510 UT, C4 and C1 were separated by 0.4 deg. ILAT, C4 and C2 by 1.9 deg. ILAT and C4 and C3 by 3.7 deg. ILAT.

2.2. Interplanetary Conditions

[10] The magnetic field and solar wind plasma parameters on 23 September 2004 are presented on Figure 2. ACE measurements (propagated to the nose of the bow shock) were provided by Omniweb at NSSDC. A 10-min delay was added to these data to take into account the propagation from the bow shock to the midaltitude cusp. Figure 2 presents the three components of the IMF in GSM, along with the density, velocity and solar wind dynamic pressure. Before 1521 UT, the IMF B_z was negative, around -3 nT, with B_y oscillating around 0, and B_x positive, around 2 nT.

After that time, a sharp turn of the IMF occurred, with B_z becoming positive, around 2 nT, B_y negative around -4 nT, and B_x around 0. Therefore the IMF was southward during the first part of the cusp crossing and then turned northward with B_y dominating for the second part of the crossing.

[11] During the same period, the solar wind density and velocity were rather stable around 4 cm^{-3} and 440 km/s respectively and increased slightly around 4.5 cm^{-3} and 460 km/s after 1526 UT. Note that the slight increase occurred about 5 min after the IMF turning. The solar wind dynamic pressure showed an increase from 1.3 nPa to 1.6 nPa.

2.3. Cluster Observations

[12] Figure 3 displays the ion and electron precipitations observed on the four Cluster spacecraft between 1505 UT and 1545 UT on 23 September 2004. The three top panels show C4, C1 and C3 omnidirectional ion spectrograms, whereas the following four panels show the downgoing (antiparallel) electron spectrograms from C4, C1, C2, and C3. The spacecraft are ordered from top to bottom as they crossed the cusp. C4 was first to enter the cusp at 1510:03 UT (77.7 ILAT, 11.2 MLT), characterized by the sharp drop of electron flux for energies above 1 keV (Figure 3d, vertical line) of plasma sheet origin and the enhancement of electrons flux below 500 eV of solar wind origin. The ion spectrogram from C4 (Figure 3a) shows energy dispersion that decreases as invariant latitude is increasing. This is a typical signature of the occurrence of reconnection at the dayside magnetosphere during periods of southward IMF [Reiff *et al.*, 1977]. C1 is the second spacecraft to enter the cusp at 1512:54 UT (78.0 ILAT and 11.2 MLT). Ions and electrons seen by C1 have about the same characteristics as those observed during the crossing of the cusp by C4. They are marked by a sharp increase of solar wind plasma and an ion dispersion that shows that their energy decreases as invariant latitude increases. Detailed examination of the ion dispersion observed by C4 and C1 shows exactly the same substructures within the dispersion, indicating a stable injection process over a timescale of around 2 min. Short bursts of low energy electrons are visible during the 2 min before the entry of C1 in the cusp, indicating that the spacecraft could have briefly entered the cusp. This is most likely resulting from a rapid toward and away motion of the cusp over the spacecraft. This feature was not observed by C4. The third spacecraft, C2, entered the cusp at 1516:37 UT (77.4 ILAT, 11.2 MLT). Only the electron spectrogram (Figure 3f) is shown since the ion instrument was off. The cusp is very similar to the previous crossings (Figures 3d and 3e) with a peak in flux around the center of the cusp.

[13] Finally the last spacecraft, C3, entered the cusp at 1523:30 UT (77.2 ILAT, 11.2 MLT). For this spacecraft the cusp appeared very different (Figure 3g): the duration of its crossing is much longer (between 1523:30 and 1539:30 UT) and it has a larger extent in latitude (between 77.2 and 81 ILAT). This is particularly visible on the electron spectrograms if we compare Figure 3g with Figures 3d, 3e, and 3f. The ion spectrogram reveals a totally different dispersion signature than observed by the previous spacecraft. First the energy of the ions decreases with increasing latitude between 1525 and 1528 UT. Then the low-energy cutoff of the ions stays at about the same energy between 1528 and 1532 UT, followed by an increase, although with

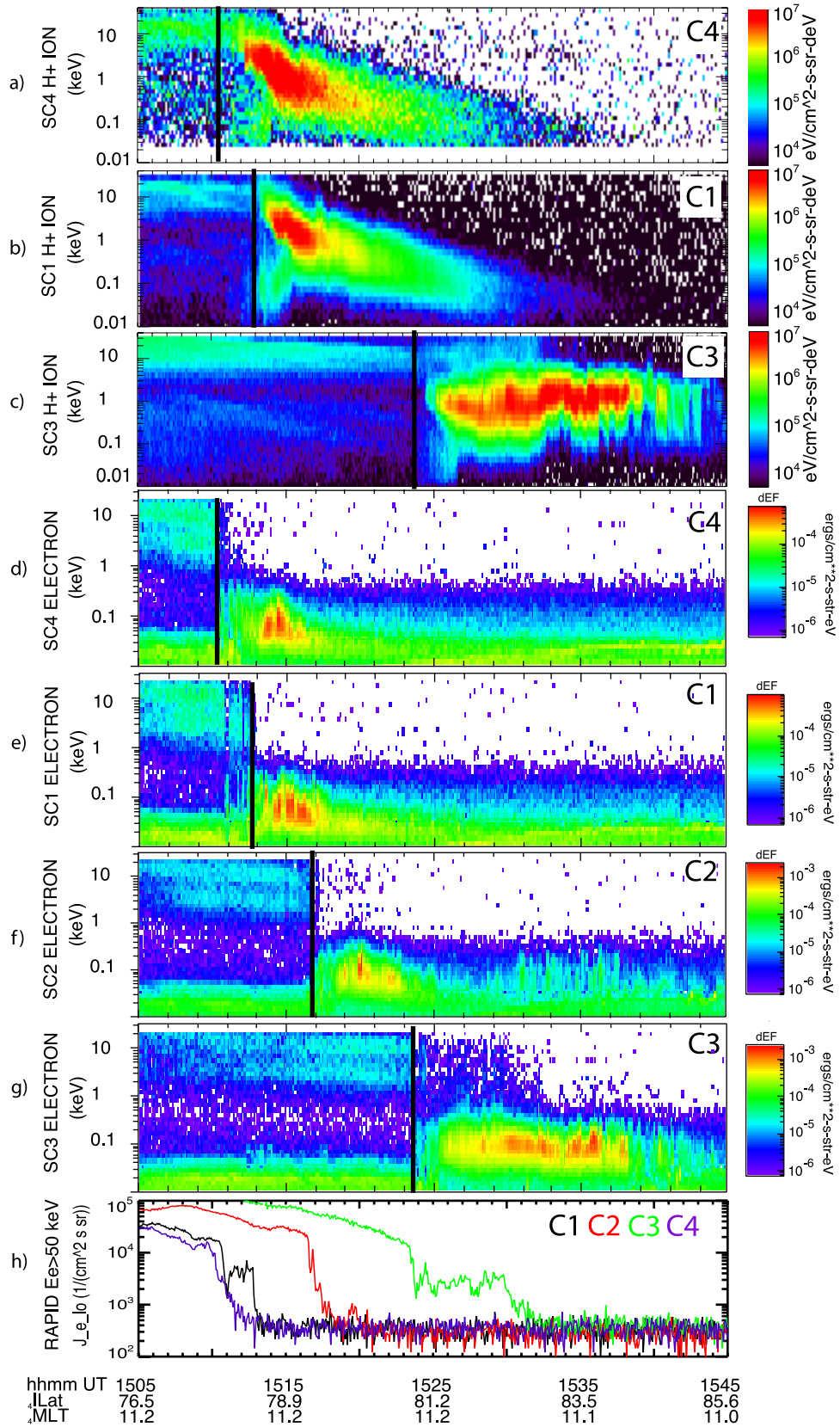


Figure 3. Omidirectional ion (CIS) and downgoing electron (PEACE) spectrograms on (a, d) C4, (b, e) C1, (f) C2, and (c, g) C3. Open-closed boundary is indicated by the vertical line on the electron spectrograms and copied on the ion spectrograms. The last panel shows the integrated flux of electrons (RAPID) between 50 and 400 keV from the four spacecraft.

some short variations up and down, between 1532 and 1539 UT. This last dispersion is typical of northward IMF conditions [Burch *et al.*, 1980]. Note that the flux of ions in the poleward dispersion between 1525 and 1528 UT shows a lower flux and lower maximum energy as compared to the dispersions observed before on C4 and C1. In addition, low fluxes of high-energy ions (above 10 keV) between 1525 and 1532 UT (Figure 3c) and low fluxes of energetic electrons, above 1 keV (Figure 3g) are also present.

[14] The integrated flux of electron between 50 and 400 keV gives an additional indication of closed and open field lines in Figure 3h. We note that as they enter the cusp, all four spacecraft show a sharp drop of the flux of energetic electrons. On C2 and C4, the drop is almost two orders of magnitude from 2×10^4 to $4 \times 10^2 \text{ cm}^{-2} \text{ s}^{-1} \text{ sr}^{-1}$. On C1, there is a first drop at 1506 and then a second one at 1513 UT. This may be due to the motion of the cusp back and forth across the spacecraft between the two drops, also indicated by the brief appearance of low energy electrons in Figure 3e. The final entry of C1 in the cusp occurs around 1513 UT. At C3, the initial flux drop is observed at 1524 UT, after which the flux stayed at an intermediate value around $3 \times 10^2 \text{ cm}^{-2} \text{ s}^{-1} \text{ sr}^{-1}$ until 1530 UT, after that time, the flux reduces until reaching the background level at 1532 UT. The region of intermediate energetic electron flux is coincident with the region of low flux of electrons above 1 keV (Figure 3g) and ions above 10 keV (Figure 3c). This region is a mix of closed and open field lines and we therefore denote it the boundary layer.

[15] To investigate the evolution of the cusp in space, we show in Figure 4 the three ion spectrograms as a function of invariant latitude. Between C4 and C1, separated by about 3 min in time, the polar cusp position did not change significantly. The main ion precipitation (indicated by the red flux levels in two top panels) occurs between 78.5 and 79.5 deg. ILAT. It is at slightly lower latitude on C1. On the other hand the OCB given by the electron (vertical line), is slightly poleward on C1 (78.0 ILAT) than on C4 (77.7 ILAT). The cusp observed 20 min later on C3 is wider in latitude. The start of ion precipitation is around 77.6 ILAT and the end around 81 ILAT. Hence the cusp has tripled its size in latitude, from 1 deg. ILAT to about 3.4 deg. ILAT. This is also clearly visible in the density measurements (three bottom panels). The region where the density is above 6 cm^{-3} is narrow on C4 and C1, yet much wider on C3. Note that the equatorward side of the cusp or boundary layer, between 77.6 ILAT and 79.5 ILAT, is as dense as the region of main cusp precipitation, between 79.5 and 81 ILAT. Only the maximum, around 14 cm^{-3} , is higher in the cusp than in the boundary layer (11 cm^{-3}).

[16] The dispersion seen in the boundary layer on C3 around 78 ILAT is characterized by a decrease of the low-energy cutoff with increasing latitude, similar to C4 and C1. However, the flux of ions between 100 eV and 1 keV is lower and the high-energy cutoff increases from about 2 keV at 77.5 ILAT to about 8 keV at 79 ILAT. Conversely the high-energy cutoff on C4 and C3 decreases from 10 keV at 78.5 ILAT to 2 keV at 79–79.5 ILAT.

[17] To get a handle on the generation mechanisms, we compare the ion dispersion observed with C1 with the one observed by C3 in the boundary layer. Figure 5 shows the downgoing and upgoing ions detected by C1 and C3. We

use the HIA detector to make a more consistent comparison between two spacecraft. The cusp precipitation observed on C1 is predominantly in the downward direction, toward the ionosphere, between 1514 and 1516 UT (Figure 5a). The ratio of the energy of the cutoff of the downgoing versus upgoing ions [Onsager *et al.*, 1995; Fuselier *et al.*, 2000; Trattner *et al.*, 2005b; Escoubet *et al.*, 2008], between 1514 UT and 1516 UT, gives an altitude of injection of $11.4 R_E$ above the spacecraft. If we add $4.5 R_E$ for the altitude of C1, the source is around a distance of $16 R_E$ along the magnetic field line. This is in good agreement with an injection on the dayside of the magnetopause around the subsolar point. After 1516 UT, the ions are mainly in the upward direction (Figure 5b), the ions having bounced in the ionosphere and moving upward out of the cusp into the plasma mantle [Rosenbauer *et al.*, 1975]. Note that the high-energy cutoff is also decreasing as latitude increases from about 10–20 keV at 1513 UT to 2 keV at 1516 UT (Figure 5a).

[18] We note that the ion dispersion in the boundary layer observed on C3 between 1525 and 1532 UT, shows higher flux in the upgoing direction (Figure 5d) than in the downgoing direction (Figure 5c). The low-energy cutoff is slightly higher in the upgoing than in the downgoing direction, which results in an unrealistic (negative) altitude of injection. A likely explanation is that the upgoing and downgoing ions were not emitted from the same source at the same time. The high-energy cutoff is also different from the one observed by C1, in this case it is increasing as the latitude increases from 1 to 2 keV at 1525 (Figure 5c) to about 5 keV at about 1529 UT. Later on in the ion precipitation observed by C3 (after 1533 UT) the downgoing ions are again dominant and the upgoing component have the highest-energy cutoff. In this case, between 1533 and 1538 UT, the distance to the site of injection is computed to be $33 R_E$ on average.

2.4. Magnetohydrodynamic Model: Global Magnetohydrodynamic Simulation

[19] A three-dimensional magnetohydrodynamic (MHD) simulation [e.g., Berchem *et al.*, 1993] of the event was carried out using the solar wind parameters and IMF measured by the ACE spacecraft as input. The results for southward IMF (1510 UT) and northward IMF (1528 UT) are shown in Figures 6a and 6b, respectively. Figure 6a is a composite picture of two- and three-dimensional renderings of the dayside magnetosphere viewed from the Sun. The backdrop of the picture is a two-dimensional cross section (Y–Z plane) of the magnetotail taken at $x = -10 R_E$ showing color contours of the plasma beta. The magnetotail lobes are readily associated with the regions of low-beta plasma (deep blue contours) separated by the high-beta plasma of the plasma sheet (gold contours) and bounded by the magnetopause (transition between blue and green contours). Three-dimensional isosurfaces of plasma beta ($= 100$) complete the picture with the same color-coding as that of the cross section contours. They indicate the presence of two regions of low magnetic field at the magnetopause. The most prominent one extends from dawn to the dusk at midlatitude whereas the other one is located in the subsolar magnetopause. Magnetic field lines threading these two regions are displayed. Open and unconnected magnetosheath magnetic field lines are shown in yellow and red,

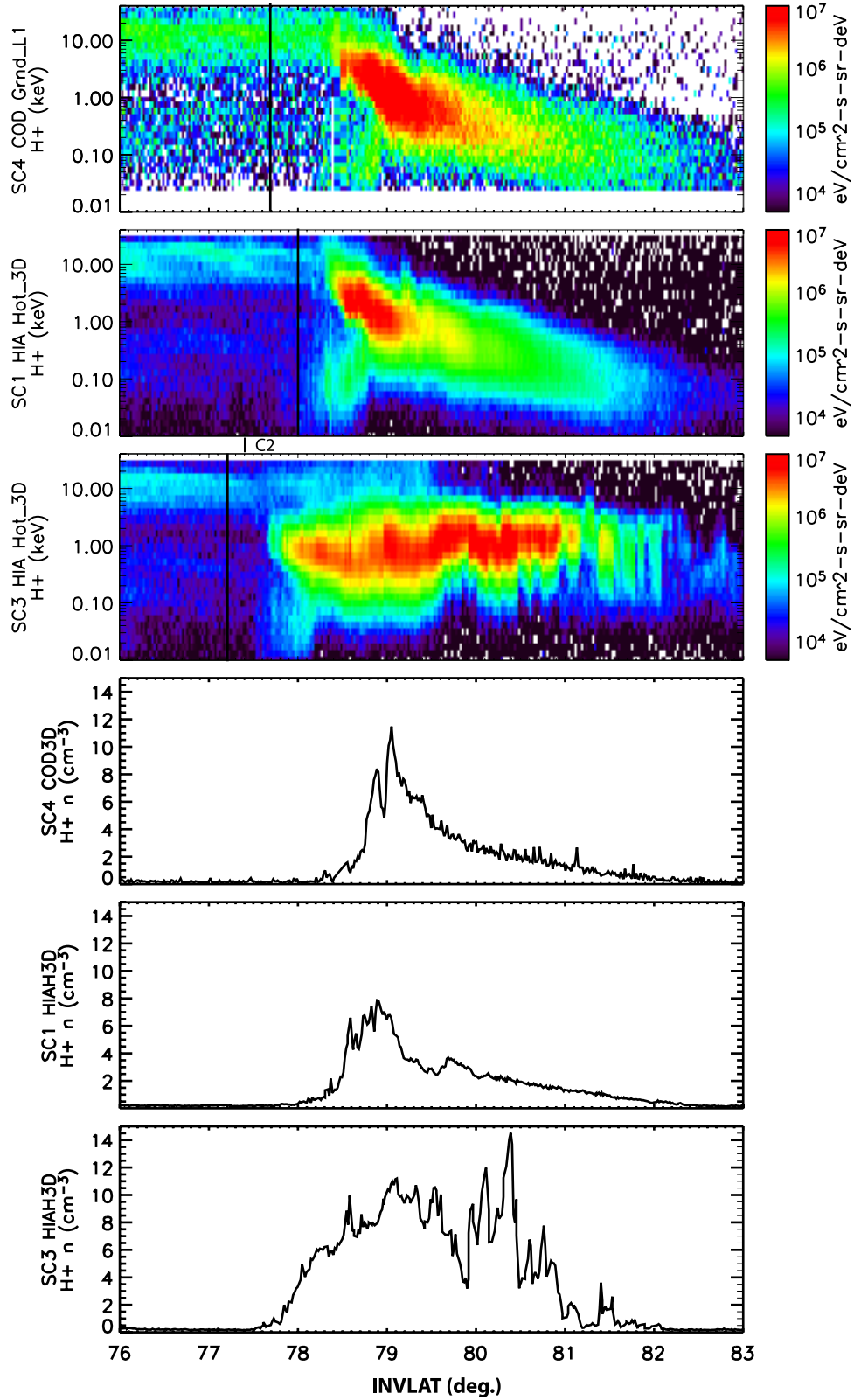


Figure 4. Omnidirectional ion spectrograms as a function of invariant latitude for (a) C4, (b) C1, and (c) C3. The OCB defined by the electrons is marked by a solid vertical line (C2 OCB has been added between C1 and C3 panels). The last three panels show the ion density from (d) C4, (e) C1, and (f) C3.

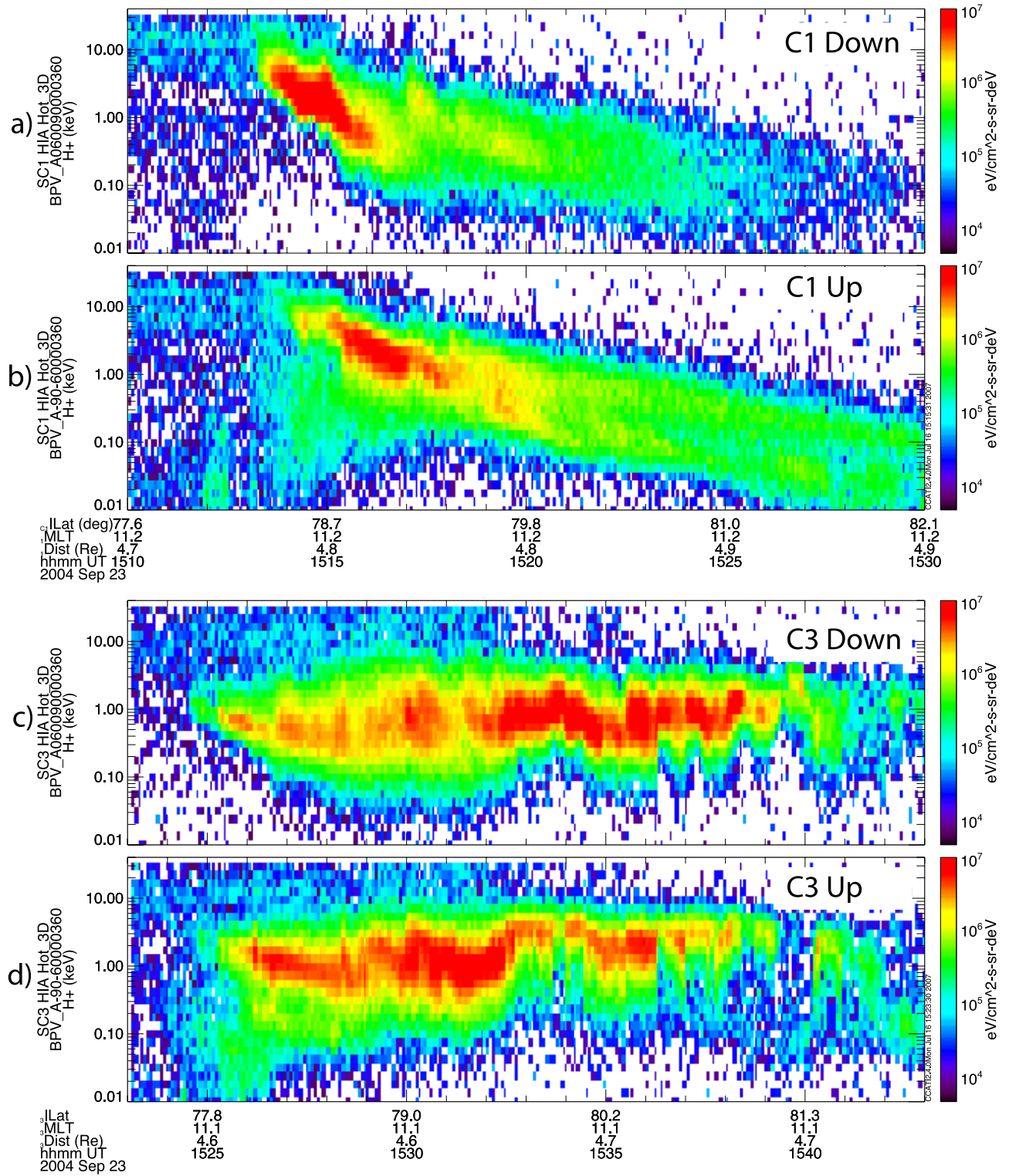


Figure 5. Omnidirectional spectrograms of (a, c) downgoing and (b, d) upgoing ions on C1 and C3, respectively. The downgoing and upgoing ions are defined within ± 30 deg around the parallel and antiparallel direction of the magnetic field.

respectively. The sharp kinks observed in the open field lines indicate the occurrence of reconnection in both regions. In particular, this configuration indicates that during the crossing of the cusp by C4, C1, and most of C2,

reconnection is taking place around the subsolar region and then the field lines (yellow lines) are pulled toward the northern and southern cusp by the magnetic tension. Under the velocity filter effect, the high-energy ions (>1 keV) will

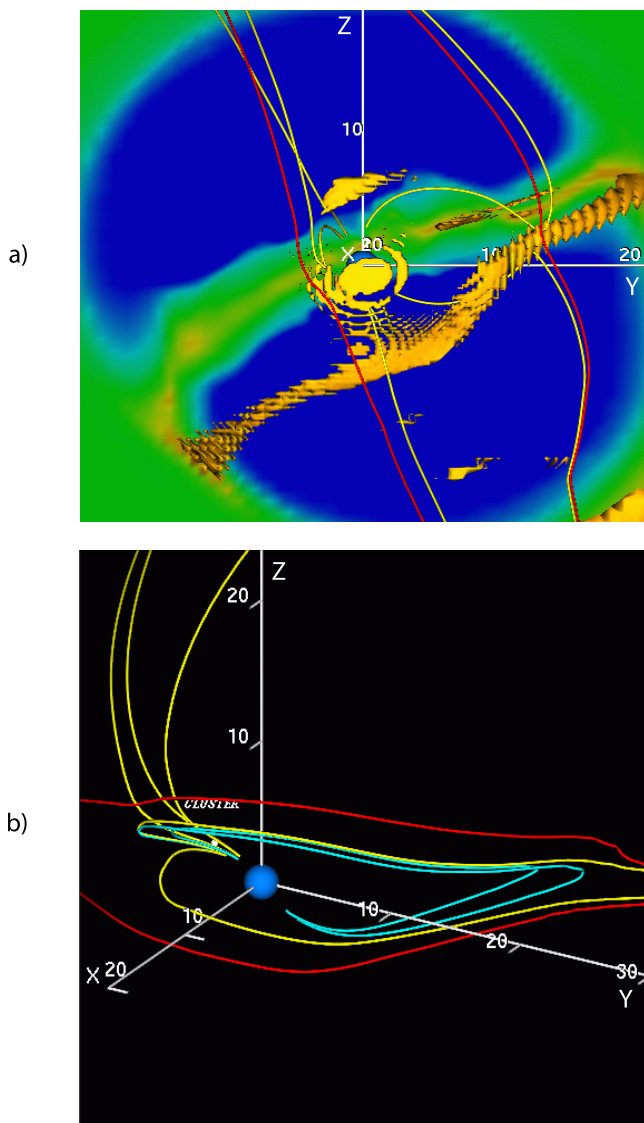


Figure 6. MHD simulation on 23 September 2004. (a) At 1510 UT when IMF- B_z is southward. Field lines from the solar wind are shown in red and field lines reconnected and opened in yellow. (b) At 1528 UT after the turning of IMF- B_z northward with dominant B_y negative, IMF field lines are in red, open field lines in yellow, and closed field lines in blue.

reach first the midaltitude cusp, and then the energy of the ions will decrease gradually as the field line is moving poleward. This is what is indeed observed on C4 and C1 (Figure 4).

[20] Figure 6b shows a snapshot of the simulation for time 1528 UT as the IMF has turned northward, with a strong dominant B_y . The magnetosphere is viewed from 2 o'clock past noon local time. Magnetic field lines have been traced using the same color-coding than before: red, yellow, and turquoise indicate unconnected, open, and closed field lines, respectively. They reveal that reconnection is now taking place around the dawn flank/lobe, poleward of the cusp. After reconnection, open field lines are now pulled sunward and toward dusk. This new

configuration suggests that high-energy ions are now injected around the poleward boundary of the cusp and that their energy gradually decrease as the invariant latitude decreases. This is what is observed between 79.5 and 81 ILAT on C3 (Figure 4). In a second step, newly open field lines from the north hemisphere reconnect a second time on the dusk flank, with open field lines coming from the south hemisphere, to form new closed field lines (blue lines). Note that the open field lines (yellow) that extend from the northern lobe to the dusk side are overdraped field lines [Crooker, 1992].

3. Discussion and Conclusions

[21] Cluster observations have revealed changes in the characteristics of the midaltitude polar cusp during an abrupt turning of the IMF from southward to northward. Under southward IMF, the first two Cluster spacecraft observed typical ion energy dispersion signatures with decreasing energy as latitude increased. A few minutes after the IMF turned northward, with a dominant azimuthal component, the last spacecraft, C3, observed a much wider cusp with first a dispersion with a decreasing energy with increasing latitude in the boundary layer and then, as C3 moved poleward, a reversed dispersion with energy increasing with increasing latitude. Furthermore the flux of high-energy ions (above 10 keV) and high-energy electrons (>above 1 keV) increased in the boundary layer, though these energetic electrons are not present when the reversed dispersion was observed poleward.

[22] We now investigate the time delay needed to change the cusp precipitation after the turning of the IMF. Following an IMF rotation, Greenwald *et al.* [1990] observed changes in the flow measured by HF radars after a few minutes and a complete reconfiguration of the convection within 6 min. Etemadi *et al.* [1988] showed that the westward flows of the dusk cell responded with a delay of 3.9 ± 2.2 min to changes in the north–south field at the subsolar magnetopause. In our case, the IMF turned northward at 1522 UT (Figure 2) and the entry of C3 in the cusp occurred at 1523:30, as determined by the electrons, and the first ions detected by C3 at 1524:30. We therefore find a delay of 1 min 30 s to 2 min 30 s. Although we have used the high-resolution OMNI data set that uses “phase front” propagation, there could be an error of a few minutes in the propagation of the IMF from the ACE position to the magnetosphere. Furthermore C2 showed very similar cusp characteristic as C4 and C3 (c.f. Figure 3: no electrons above 1 keV in the cusp), and cusp exit was around 1523 UT which are good indications that the effect of IMF turning had not yet manifested in the midaltitude cusp.

[23] Sandholt *et al.* [2002] reported changes in the cusp seen in ground optical data and with DMSP satellite following a strong bipolar signature of the IMF from south to north (-20 nT to $+20$ nT). They observed a time delay of 2 min before the apparition of a northward IMF type aurora and “V” shape ion dispersion in agreement with our observations. A difference from our case is the presence of an auroral arc of about 4 keV near the poleward boundary of the cusp. This could be due to the very different IMF conditions (IMF B_z changing from -20 nT to $+20$ nT in their case against B_z changing from -4 to $+3$ nT in our

case). Alternatively, the higher altitude of observation in our case ($3.7 R_E$ in our case and around 800 km in their case) could mean that we are above the region where electrons are accelerated.

[24] When the IMF is northward the ion dispersion has a “V” shape [Reiff *et al.*, 1977; Burch *et al.*, 1980; Woch and Lundin, 1992]. In this study we observe a “V” shaped dispersion after the turning of the IMF northward. However, this “V” is far from being symmetric. We see high-energy ions (>10 keV) and high-energy electrons (>1 keV) in the equatorward part of the “V.” This flux level is however intermediate between closed field lines and open field lines in the cusp (Figure 3h). This suggests that these field lines were closed before and recently opened or previously open and recently closed. If they were closed before and recently opened, one would expect that the energetic electrons (above 50 keV) would have disappeared and we would not observe them at C3 during the 6 min it moved poleward. In addition C4, C1, and C2 observed the cusp on open field lines at the same invariant latitude down to about 7 min before C3 observations of the intermediate high-energy particle flux (Figure 4); the open closed boundary (OCB) would have to move by more than 2 deg poleward with field lines becoming open in about 7 min. This motion would be more than twice as fast as typically observed, around 0.12 deg/min [Escoubet *et al.*, 2006; Pitout *et al.*, 2006a]. Therefore the alternative explanation that the field lines were opened and then closed is most likely. The MHD simulation (Figure 6b) showed first that the field lines were open on the dawn lobes and then closed on the dusk flank. In such case there is no need to suggest the motion of the OCB. In fact if we assume that the old OCB is indicated by the first drop of the energetic electrons (vertical line on Figure 4c), then it is very close to the one observed on C2 before the change of the IMF.

[25] The right side of the “V” is produced by the reconnection between the northward-dawnward IMF and the dawn lobes, creating a tension in the magnetic field that pulls the field line both sunward and duskward (these flows are indeed observed by C3, but not shown). This motion produces the velocity filter effect on the ions and the energy decreases as the latitude decreases. By opposition to the southward IMF dispersion, this right side of the “V” is not smooth (Figure 5c). The low energy threshold varies between 200 and 800 eV and is most likely due to oscillations of the position of the reconnection line with respect to the slow motion of the spacecraft. Alternatively it could also be due to a varying reconnection rate that creates jumps in energy [Lockwood and Smith, 1992; Newell and Meng 1995]. This is however not something we can check in this study, since when C3 observed these oscillations the other spacecraft were already in the polar cap.

[26] After being reconnected and ions injected in the cusp (right side of “V”), field lines reconnect on the dusk flank with another field lines from the southern hemisphere [Crooker, 1992; Watanabe *et al.*, 2006]. After that there is no injection of solar wind plasma since the field lines are closed, the flux of downgoing ions is therefore lower than the upgoing (which are now bouncing from the mirror point) ions (Figures 5c and 5d). High energy particle coming from the nightside plasma sheet can now drift on

these closed field lines and start to refill them with magnetospheric plasma.

[27] It is not clear how to get the dispersion itself in the left side of the “V” which is in fact more a widening of the energy band (the low-energy cutoff is decreasing and the high-energy cutoff is increasing). Maybe as the field line is moving more along the flank down the tail, the magnetosheath plasma present on this field line has less and less access to the ionosphere or more is being lost and we have in fact just a regular decrease of the flux of particles (Figure 6). Further simulations with individual particles may help to understand these signatures.

[28] **Acknowledgments.** We thank Joe King and Natalia Papatashvili, NSSDC; N. F. Ness, Bartol Research Institute, USA; and McComas, SWRI, USA for the provision of solar wind data. M. Fraenz is acknowledged for the development of CCAT1 to plot the ion CIS data. Research at UCLA was supported by NASA grants NNX07AG62G and NNG05GK91G and NSF grant ATM-0603222. The work at Lockheed Martin was supported by NASA contracts NNG05GE93G and a grant by the National Science Foundation under grant 0503201.

[29] Amitava Bhattacharjee thanks Per Sandholt and Larry Lyons for their assistance in evaluating this paper.

References

- Berchem, J., J. Raeder, and M. Ashour-Abdalla (1993), Mission-oriented simulations of small and large scale structures in the dayside magnetosphere, in *Spatio-Temporal Analysis for Resolving Plasma Turbulence (START)*, edited by C. P. Escoubet, *Eur. Space Agency Spec. Publ., ESA SP WPP-047*, 393.
- Bosqued, J. M., et al. (2005), Multipoint observations of transient reconnection signatures in the cusp precipitation: A Cluster-IMAGE detailed case study, *J. Geophys. Res.*, *110*, A03219, doi:10.1029/2004JA010621.
- Burch, J. L. (1973), Rate of erosion of dayside magnetic flux based on a quantitative study of the dependence of polar cusp latitude on the interplanetary magnetic field, *Radio Sci.*, *8*(11), 955–961, doi:10.1029/RS008i011p00955.
- Burch, J. L., P. H. Reiff, R. W. Spiro, R. A. Heelis, and S. A. Fields (1980), Cusp region particle precipitation and ion convection for northward interplanetary magnetic field, *Geophys. Res. Lett.*, *7*, 393–396, doi:10.1029/GL007i005p00393.
- Carbary, J. F., and C.-I. Meng (1986), Relations between the interplanetary magnetic field B_z , AE index, and cusp latitude, *J. Geophys. Res.*, *91*, 1549–1556, doi:10.1029/JA091iA02p01549.
- Crooker, N. U. (1992), Reverse convection, *J. Geophys. Res.*, *97*, 19,363–19,372, doi:10.1029/92JA01532.
- Eather, R. H. (1985), Polar cusp dynamics, *J. Geophys. Res.*, *90*, 1569–1576, doi:10.1029/JA090iA02p01569.
- Escoubet, C. P., and J. M. Bosqued (1989), The influence of IMF- B_z and/or AE on the polar cusp: An overview of observations from the AUREOL-3 satellite, *Planet. Space Sci.*, *37*, 609–626, doi:10.1016/0032-0633(89)90100-1.
- Escoubet, C. P., M. F. Smith, S. F. Fung, P. C. Anderson, R. A. Hoffman, E. M. Basinska, and J. M. Bosqued (1992), Staircase ion signature in the polar cusp: A case study, *Geophys. Res. Lett.*, *19*, 1735–1738, doi:10.1029/92GL01806.
- Escoubet, C. P., M. Fehring, and M. Goldstein (2001), The Cluster mission, *Ann. Geophys.*, *19*, 1197–1200.
- Escoubet, C. P., et al. (2006), Temporal evolution of a staircase ion signature observed by Cluster in the mid-altitude polar cusp, *Geophys. Res. Lett.*, *33*, L07108, doi:10.1029/2005GL025598.
- Escoubet, C. P., et al. (2008), Two sources of magnetosheath ions observed by Cluster in the mid-altitude polar cusp, *Adv. Space Res.*, doi:10.1016/j.asr.2007.04.031, in press.
- Ettemadi, A., S. W. H. Cowley, M. Lockwood, B. J. I. Bromage, D. M. Willis, and H. Lühr (1988), The dependence of high-latitude dayside ionospheric flows on the north–south component of the IMF: A high time resolution correlation analysis using the EISCAT POLAR and AMPTE UKS and IRM data, *Planet. Space Sci.*, *36*, 471–498, doi:10.1016/0032-0633(88)90107-9.
- Frank, L. A. (1971), Plasma in the Earth’s polar magnetosphere, *J. Geophys. Res.*, *76*, 5202–5219, doi:10.1029/JA076i022p05202.
- Fuselier, S. A., S. M. Petrincec, and K. J. Trattner (2000), Stability of the high-latitude reconnection site for steady northward IMF, *Geophys. Res. Lett.*, *27*, 473–476, doi:10.1029/1999GL003706.

- Greenwald, R. A., K. B. Baker, J. M. Ruohoniemi, J. R. Dudeney, M. Pinnock, N. Mattin, J. M. Leonard, and R. P. Lepping (1990), Simultaneous conjugate observations of dynamic variations in high-latitude dayside convection due to changes in IMF B_y , *J. Geophys. Res.*, *95*, 8057–8072, doi:10.1029/JA095iA06p08057.
- Heikkila, W. J., and J. D. Winningham (1971), Penetration of magnetosheath plasma to low altitudes through the dayside magnetospheric cusps, *J. Geophys. Res.*, *76*, 883–891, doi:10.1029/JA076i004p00883.
- Johnstone, A. D., et al. (1997), PEACE: A plasma electron and current experiment, *Space Sci. Rev.*, *79*, 351–398, doi:10.1023/A:1004938001388.
- Lockwood, M., and M. F. Smith (1992), The variation of reconnection rate at the dayside magnetopause and cusp ion precipitation, *J. Geophys. Res.*, *97*, 14,841–14,847, doi:10.1029/92JA01261.
- Newell, P. T., and C.-I. Meng (1991), Ion acceleration at the equatorward edge of the cusp: Low-altitude observations of patchy merging, *Geophys. Res. Lett.*, *18*, 1829–1832, doi:10.1029/91GL02088.
- Newell, P., and C. Meng (1994), Ionospheric projections of magnetospheric regions under low and high solar wind pressure conditions, *J. Geophys. Res.*, *99*, 273–286, doi:10.1029/93JA02273.
- Newell, P. T., and C.-I. Meng (1995), Cusp low-energy ion cutoffs: A survey and implications for merging, *J. Geophys. Res.*, *100*, 21,943–21,952, doi:10.1029/95JA01608.
- Onsager, T. G., S.-W. Chang, J. D. Perez, J. B. Austin, and L. X. Janoo (1995), Low-altitude observations and modeling of quasi-steady magnetopause reconnection, *J. Geophys. Res.*, *100*, 11,831–11,844, doi:10.1029/94JA02702.
- Pitout, F., C. P. Escoubet, Y. V. Bogdanova, E. Georgescu, A. N. Fazakerley, and H. Rème (2006a), Response of the mid-altitude cusp to rapid rotations of the IMF, *Geophys. Res. Lett.*, *33*, L11107, doi:10.1029/2005GL025460.
- Pitout, F., C. P. Escoubet, B. Klecker, and H. Rème (2006b), Cluster survey of the mid-altitude cusp: 1. Size, location, and dynamics, *Ann. Geophys.*, *24*, 3011–3026.
- Reiff, P. H., J. L. Burch, and T. W. Hill (1977), Solar wind plasma injection at the dayside magnetospheric cusp, *J. Geophys. Res.*, *82*, 479–491, doi:10.1029/JA082i004p00479.
- Reiff, P. H., J. L. Burch, and R. W. Spiro (1980), Cusp proton signatures and the interplanetary magnetic field, *J. Geophys. Res.*, *85*, 5997–6005, doi:10.1029/JA085iA11p05997.
- Rème, H., et al. (2001), First multispacecraft ion measurements in and near the earth's magnetosphere with the identical Cluster ion spectrometry (CIS) experiment, *Ann. Geophys.*, *19*, 1303–1354.
- Rosenbauer, H., H. Grünwaldt, M. D. Montgomery, G. Paschmann, and N. Sckopke (1975), Heos 2 plasma observations in the distant polar magnetosphere: The plasma mantle, *J. Geophys. Res.*, *80*, 2723–2737, doi:10.1029/JA080i019p02723.
- Sandholt, P. E., et al. (1994), Cusp/cleft auroral activity in relation to solar wind dynamic pressure, interplanetary magnetic field B_z and B_y , *J. Geophys. Res.*, *99*, 17,323–17,342, doi:10.1029/94JA00679.
- Sandholt, P. E., C. J. Farrugia, J. Moen, and W. F. Denig (2002), The cusp in rapid transition, *J. Geophys. Res.*, *107*(A12), 1427, doi:10.1029/2001JA009214.
- Trattner, K. J., et al. (2003), Cusp structures: Combining multi-spacecraft observations with ground-based observations, *Ann. Geophys.*, *21*, 2031–2041.
- Trattner, K. J., S. A. Fuselier, T. K. Yeoman, C. Carlson, W. K. Peterson, A. Korth, H. Rème, J. A. Sauvaud, and N. Dubouloz (2005a), Spatial and temporal cusp structures observed by multiple spacecraft and ground based observations, *Surv. Geophys.*, *26*, 281–305, doi:10.1007/s10712-005-1883-3.
- Trattner, K. J., S. A. Fuselier, S. M. Petrinec, T. K. Yeoman, C. Mouikis, H. Kucharek, and H. Rème (2005b), Reconnection sites of spatial cusp structures, *J. Geophys. Res.*, *110*, A04207, doi:10.1029/2004JA010722.
- Tsyganenko, N. A., and D. P. Stern (1996), Modeling the global magnetic field of the large-scale Birkeland current systems, *J. Geophys. Res.*, *101*, 27,187–27,198.
- Watanabe, M., G. J. Sofko, D. A. André, J. M. Ruohoniemi, M. R. Hairston, and K. Kabin (2006), Ionospheric signatures of internal reconnection for northward interplanetary magnetic field: Observation of “reciprocal cells” and magnetosheath ion precipitation, *J. Geophys. Res.*, *111*, A06201, doi:10.1029/2005JA011446.
- Wilken, B., et al. (2001), First results from the RAPID imaging energetic particle spectrometer on board Cluster, *Ann. Geophys.*, *19*, 1355–1366.
- Woch, J., and R. Lundin (1992), Magnetosheath plasma precipitation in the polar cusp and its control by the interplanetary magnetic field, *J. Geophys. Res.*, *97*, 1421–1430, doi:10.1029/91JA02487.
- Yamauchi, M., R. Lundin, and T. A. Potemra (1995), Dynamic response of the cusp morphology to the interplanetary magnetic field changes: An example observed by Viking, *J. Geophys. Res.*, *100*, 7661–7670, doi:10.1029/95JA00333.
- Zhou, X. W., C. T. Russell, G. Le, S. A. Fuselier, and J. D. Scudder (2000), Solar wind control of the polar cusp at high altitude, *J. Geophys. Res.*, *105*, 245–251, doi:10.1029/1999JA900412.

J. Berchem, Institute of Geophysics and Planetary Physics, University of California, Los Angeles, 405 Hilgard Avenue, Los Angeles, CA 90095-1567, USA.

J.-M. Bosqued, I. Dandouras, and H. Rème, Centre d'Etude Spatiale des Rayonnements, 9 Avenue du Colonel Roche, B. P. 4346, F-31028, Toulouse Cedex 4, France.

P. W. Daly, Max Planck Institute for Solar System Research, Max-Planck-Str. 2, D-37191 Katlenburg-Lindau, Germany.

M. Dunlop, Rutherford Appleton Laboratory, Chilton, Didcot, Oxford OX11 0QX, UK.

C. P. Escoubet, H. Laakso, A. Masson, and M. Taylor, European Space Research and Technology Centre, European Space Agency, Postbus 299, Keplerlaan, 1, NL-2200 AG Noordwijk, Netherlands.

A. Fazakerley, Department of Physics, Mullard Space Science Laboratory, University College London, Holmbury St. Mary, Dorking, Surrey RH5 6NT, UK.

F. Pitout, Laboratoire de Planetologie de Grenoble, Batiment D de Physique, BP 53, F-38041, Saint-Martin d'Heres, France.

K. Trattner, Lockheed Martin Air Traffic Management, Dept. ADCS, Building 252, Lockheed Research Laboratories, 3251 Hanover Street, Palo Alto, CA 94304-1191, USA.